A SUPERPOSED EPOCH ANALYSIS OF GEOMAGNETIC STORMS OVER A SOLAR CYCLE

J. A. Hutchinson[1], D. M. Wright[1], S. E. Milan[1] and A. Grocott[1], [1]Radio & Space Plasma Physics, Department of Physics and Astronomy, University of Leicester, University Road, Leicester, LE1 7RH, Contact: jh251@ion.le.ac.uk.

Introduction: Geomagnetic storms are generally defined by periods of intense solar wind – magnetosphere (SW-M) coupling usually associated with extreme conditions in the solar wind (SW), such as coronal mass ejections (CMEs) or co-rotating interaction regions (CIRs). They cause large global disturbances in the Earth's magnetosphere [e.g. 1] during which, large amounts of energy are stored in the magnetotail and inner magnetosphere, producing an enhanced ring current and energizing plasma to relativistic levels through not yet fully understood excitation mechanisms [e.g. 2].

In this study we investigate the general features of storms by undertaking a superposed epoch analysis of geomagnetic storms over the last solar cycle (1997-2008) in order to investigate the correlation between SW driving conditions and the subsequent ring current enhancement seen in SYM-H evolution.

Identification of Events: By exploiting data from the Advanced Composition Explorer (ACE) spacecraft, giving upstream SW conditions at the L1 point, in conjunction with space- and ground-based measurements of geospace over the last solar cycle, a database of geomagnetic storms has been compiled and analyzed.

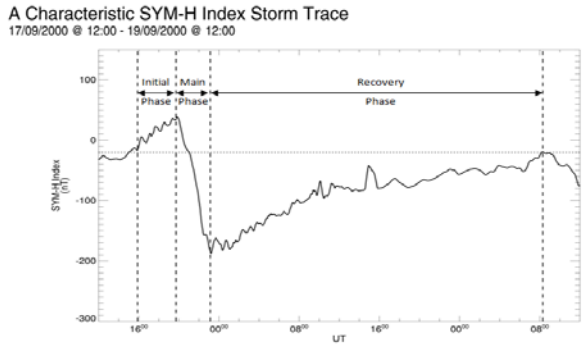

Figure 1: A characteristic SYM-H index storm trace showing initial, main and recovery phases.

Storms can be easily identified from their characteristic SYM-H variation (figure 1); a geomagnetic index giving a measure of the ring current from ground-based equatorial magnetometers showing the deflection of the terrestrial magnetic field caused by the induced, opposing magnetic field from the increased ring current [3]. After locating storms, onset mechanisms were determined as broadly associated with either CMEs or CIRs using the ACE OMNI data compared to typical signatures [4,5].

Superposition Methodology: An automated, systematic approach was taken to identify all periods of SYM-H less than -80 nT and their subsequent recovery to quiet conditions of -15 nT; with the latter taken as the end of the recovery phases. The end of the main phase was identified as the minimum value of SYM-H reached. Candidate events were then manually inspected to determine if they were correctly identified as storms, followed by manual selection of the initial and main phases based on the start of the sharp increase in SW activity and the start of the main drop in SYM-H respectively. Storms were then categorized as weak ($-150 < \text{SYM-H} \leq -80$) nT, moderate ($-300 < \text{SYM-H} \leq -150$) nT and intense ($\text{SYM-H} \leq -300$) nT.

Storms were superposed in a similar way to [6], whereby the average durations of individual storm phases (initial, main and recovery) were found for different storm size categories and onset mechanisms and then the subset of individual storm phases in that category were adjusted to the normalized phase time indices. This was done by shifting their data timestamps to ensure common points in the storm progression were superposed. The start of each phase is essentially a common reference time for the superposition, but the adjustment of individual storm phase lengths to the average of the sub-category of the parent population is vital in ensuring good alignment of the superposition. This is demonstrated in figure 2.

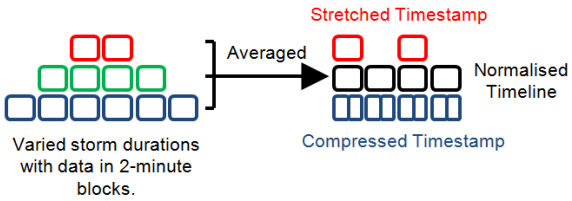

Figure 2: Diagram of superposition method, finding average periods and then adjusting timestamps of individual data to the normalized timeline. Each column is then superposed.

Observations: 143 geomagnetic storms were identified in the last solar cycle and categorized and superposed as discussed above. Generally the distribution of events was similar to previous cycles, with many more weaker storms than intense, a bi-annual distribution seen particularly in intense events, similar to [1], and a solar cycle variation that closely followed solar activity given by sunspot number.

Superposed SYM-H results. The results of the superposed SYM-H index for different storm sizes can be seen in figure 3; showing weaker storms have on average a 4x smaller ring current enhancement and are also shorter in duration. Main phase duration is seen to decrease with storm size and larger storms are more often

associated with multiple drops in main phase [e.g. 7] and other smaller events. Note fewer events are averaged in the most intense category so less smoothing occurs, seen in the grey standard error bars.

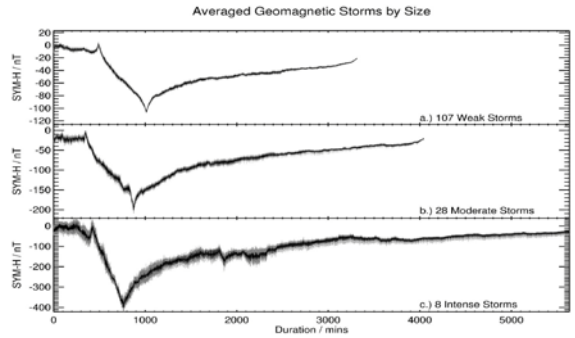

Figure 3: Superposed SYM-H storm traces, a.) Weak storms, b.) Moderate storms, c.) Intense storms, on a common time axis but varying SYM-H scales.

Superposed CME/CIR comparison. Direct comparison between CME and CIR driven storms was only possible for weak storms, as there were no large CIR driven events. This can be seen in figure 4, where again there are less CIR events averaged and larger standard error bars in grey. However it can be seen that on average, CME storms have a much shorter duration and that CIR storms are more gradual in both main and recovery phases.

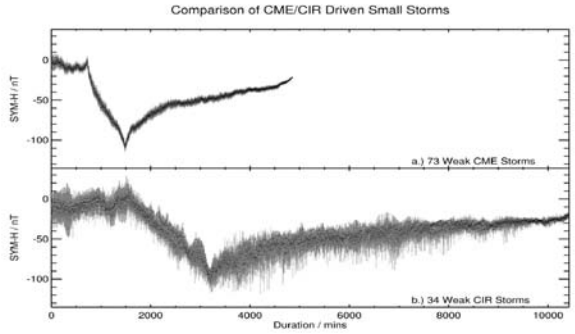

Figure 4: Superposed SYM-H traces, a.) CME driven small storms, b.) CIR driven small storms.

Main phase duration with storm size. An interesting new trend is observed in the main phase duration with storm size when compared to the results of [6]. They showed that storm duration increases with storm size, whereas in general ours is opposite. This was investigated further by re-binning data into smaller 50 nT SYM-H size bins to expand this trend further but reducing the statistical significance of each data point. This can be seen in figure 5, where the trend is seen to reverse to more intense storms having shorter durations beyond about -150 nT. Above this threshold our results quite closely match those of [6], seen in the Pearson's Correlation Coefficient of -0.817.

Recovery phase duration with storm size was shown to be very similar to that of [6] suggesting like storms were investigated and further emphasizing this new trend reversal in main phase duration. Various SW-M coupling functions were also investigated showing good correlation between SW-M coupling and storm intensity.

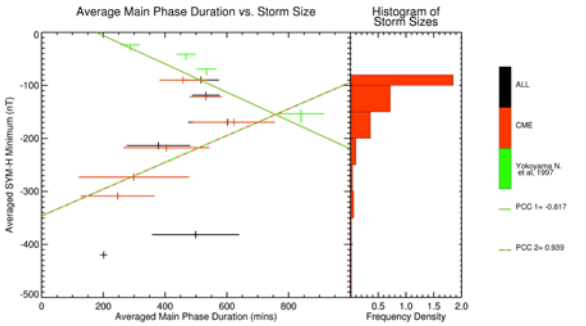

Figure 5: Average main phase duration with storm size and onset mechanism compared to previous results of [6] with least squares lines of best fit and stated Pearson's correlation coefficients.

Discussion: We have analyzed 143 geomagnetic storms in the last solar cycle using a different superposed epoch analysis that better aligns like points in the variable progression of individual storms for superposition. Direct comparison between results for weak CME and CIR storms is presented. The associated superposed SW data for each storm subcategory was also investigated, showing larger enhancements and coupling for more intense storms, as well as the strong dependence of main phase duration on the period on southward interplanetary magnetic field (IMF).

Given this dependence, it is interesting to ask why the most intense storms have on average the same main phase duration as the weakest storms and in general what causes the trend reversal in figure 5. It is suggested that the first trend is as might be expected in that it takes longer to get a more intense ring current for weak to moderate driving, but beyond that the SW conditions are so extreme that intense storms occur in much shorter timescales. It could also be that the ring current recovery rate becomes dominated by ring current enhancement mechanisms to give this trend reversal and this is the subject of current work, using auroral imagery from the IMAGE and POLAR space missions and radar data from the SuperDARN network to investigate relative energy input/dissipation rates during storm periods.

References: [1] Gonzalez W. D. et al. (1994) *JGR*, *99*(A4), 5571–5792. [2] Daglis I. A. et al. (1999) *Rev. Geophys.*, 37(4), 407–438. [3] Wanliss J. A. and Showalter K. M. (2006) *JGR*, *111*(A2). [4] Klein L. W. and Burlaga L. F. (1982) *JGR*, *87*(A2), 613-624. [5] Burlaga L. F. (1974) *JGR*, *79*(25), 3717–3725. [6] Yokoyama N. and Kamide Y. (1997) *JGR*, *102*(A7), 14215–14222. [7] Richardson I. G. and Zhang J. (2008) *Geophys. Res. Lett.*, 35(6).